iScience

CellPress
OPEN ACCESS

Article

Nanoparticle-Mediated Inhibition of Notch Signaling Promotes Mitochondrial Biogenesis and Reduces Subcutaneous Adipose Tissue Expansion in Pigs

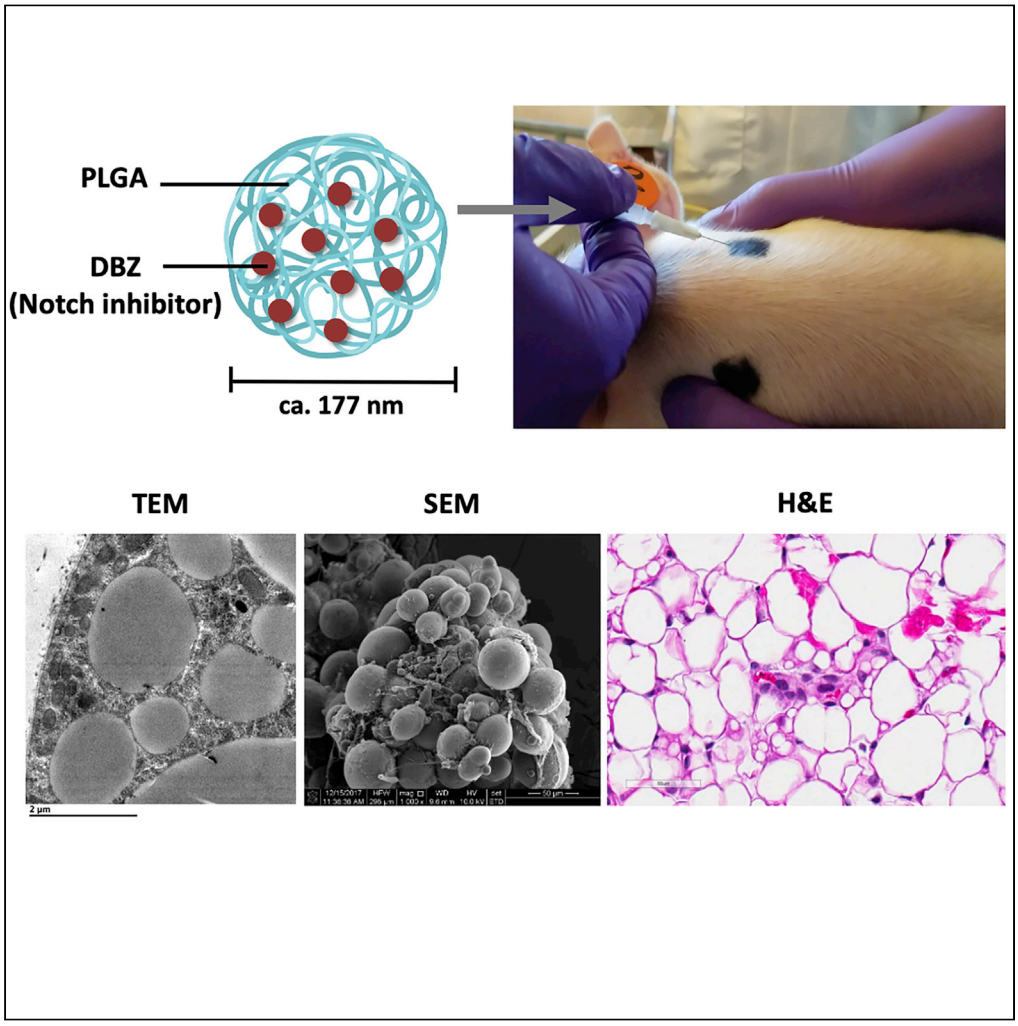

Di Huang, Naagarajan Narayanan, Mario A. Cano-Vega, Zhihao Jia, Kolapo M. Ajuwon, Shihuan Kuang, Meng Deng

skuang@purdue.edu (S.K.)
deng65@purdue.edu (M.D.)

HIGHLIGHTS

DBZ promotes beige adipogenesis and mitochondrial biogenesis in porcine adipocytes

Encapsulation of DBZ into NPs allows for efficient and sustained Notch inhibition

DBZ NPs induce upregulated beige-specific gene expression in porcine adipocytes

Local injection of DBZ NPs reduces subcutaneous adipose tissue expansion in pigs

Huang et al., iScience *23*, 101167
June 26, 2020
https://doi.org/10.1016/j.isci.2020.101167

iScience

CellPress
OPEN ACCESS

Article

Nanoparticle-Mediated Inhibition of Notch Signaling Promotes Mitochondrial Biogenesis and Reduces Subcutaneous Adipose Tissue Expansion in Pigs

Di Huang,[1,2,3] Naagarajan Narayanan,[2,3] Mario A. Cano-Vega,[2,3] Zhihao Jia,[1] Kolapo M. Ajuwon,[1] Shihuan Kuang,[1,4,*] and Meng Deng[2,3,5,6,7,*]

SUMMARY

Inhibition of Notch signaling has been shown to induce white to beige transformation of adipocytes and reduce the risk of obesity in mice. However, it remains unknown whether the metabolic benefits of Notch inhibition are dependent on uncoupling protein 1 (UCP1)-mediated thermogenesis and evolutionarily relevant in other mammalian species. Here we report the effect of Notch inhibition in adipocytes of pigs, which lost the UCP1 gene during evolution. Notch inhibition using a γ-secretase inhibitor dibenzazepine (DBZ) promoted beige adipogenesis and mitochondrial biogenic gene expression in porcine adipocytes. Moreover, encapsulation of DBZ into poly(lactide-*co*-glycolide) nanoparticles enabled rapid cellular internalization and enhanced bioactivity to achieve sustained Notch inhibition, thereby inducing beige-specific gene expression and reducing subcutaneous adipose tissue expansion in pigs. These results demonstrate for the first time a role of Notch signaling in regulating adipose plasticity in large animals, highlighting the therapeutic potential of targeting Notch signaling in obesity treatment.

INTRODUCTION

Obesity is a chronic disease involving an excessive amount of adipose tissue that increases the body weight and induces deleterious consequences for metabolic health (Pilitsi et al., 2018). Two types of adipose tissue exist in mammals, which are white adipose tissue (WAT) and brown adipose tissue (BAT). WAT principally functions in the energy storage through lipid accumulation, whereas BAT breaks down lipids to generate heat via uncoupling protein 1 (UCP1)-mediated non-shivering thermogenesis (Rosen and Spiegelman, 2006). In addition to the classic white and brown adipocytes, another metabolic phenotype, the beige (also called brite for "brown in white") adipocytes have also been identified in certain depots of WAT with similar characteristics to BAT, in particular the capacity for uncoupled respiration and breakdown of lipids (Lshibashi and Seale, 2010) (Petrovic et al., 2010) (Wu et al., 2012). Although BAT was previously considered to be restricted to infants and small animals, the recent discovery of BAT in human adults stimulated the research interests in increasing energy expenditure by activation of BAT and recruitment of beige adipocytes (termed "browning"). Browning is therefore considered a potential strategy to modulate energy balance and improve metabolic health (Kajimura and Saito, 2014) (Lidell et al., 2013).

Considerable attention has been given to the potential of increasing adipose tissue thermogenesis as a way of combating obesity development. Therapeutic perspectives can be expected from the use of pharmacotherapeutic agents that induce adipose browning, such as stimulation of BAT-specific UCP1 and enhancement of oxidative metabolism in WAT. UCP1 has long been considered a key factor in regulation of non-shivering thermogenesis and body adiposity, but one potential risk of UCP1 overexpression in WAT is excessive heat production, which may result in hyperthermia (Zheng et al., 2017) (Ost et al., 2017). The identification of UCP1-independent thermogenic mechanisms therefore attracts considerable attention in recent years. A variety of signaling pathways and genes involved in the regulatory control of beige adipocytes have been discovered with many browning agents evaluated *in vitro* or in rodent models *in vivo* (Bi et al., 2014) (Moisan et al., 2015) (Ohno et al., 2012). We have previously reported that the Notch signaling pathway is critical in regulation of adipose browning as well as energy homeostasis (Bi and Kuang, 2015). It was found that inhibition of Notch signaling through administration of a γ-secretase inhibitor

[1]Department of Animal Sciences, Purdue University, West Lafayette, IN 47907, USA

[2]Department of Agricultural and Biological Engineering, Purdue University, West Lafayette, IN 47907, USA

[3]Bindley Bioscience Center, Purdue University, West Lafayette, IN 47907, USA

[4]Center for Cancer Research, Purdue University, West Lafayette, IN 47907, USA

[5]School of Materials Engineering, Purdue University, West Lafayette, IN 47907, USA

[6]Weldon School of Biomedical Engineering, Purdue University, West Lafayette, IN 47907, USA

[7]Lead contact

*Correspondence: skuang@purdue.edu (S.K.), deng65@purdue.edu (M.D.)

https://doi.org/10.1016/j.isci.2020.101167

dibenzazepine (DBZ) resulted in browning of WAT, decreased body fat mass, and improved systemic metabolism in obese mice (Bi et al., 2014). Moreover, sustained Notch inhibition and enhanced anti-obesity therapeutic efficacy in obese mice could be further achieved through encapsulating the drug into polymeric particles (Jiang et al., 2015) (Jiang et al., 2017).

Rodent models have long been the pillar of obesity studies, because they are inexpensive to maintain, have a sequenced genome, and are easily modified by genetic engineering. However, disparate results in metabolism and physiology between rodents and humans have undoubtedly complicated the translation of fundamental research findings into therapeutic interventions for obesity (Spurlock and Gabler, 2008). Also, it remains unknown whether the metabolic benefits of Notch inhibition are dependent on UCP1-mediated thermogenesis and evolutionarily relevant in other mammalian species. The pig is emerging as an alternative biomedical model for investigating energy metabolism and obesity, particularly for UCP1-independent thermogenic mechanisms, due to the presence of excessive WAT and absence of functional BAT postnatally resulting from the lack of UCP1 protein in the domestic pig lineage (Jastroch and Andersson, 2015) (Berg et al., 2006). Furthermore, the pig also has similar metabolic features and cardiovascular system as well as proportionally similar organ sizes to humans (Spurlock and Gabler, 2008).

Herein, we report that inhibition of Notch signaling pathway promotes beige adipocyte-specific gene expression and mitochondrial biogenesis, as well as reduces adiposity in pigs *in vivo*. We chose poly(lactide-*co*-glycolide) (PLGA) as the carrier matrix, as it is a widely used polymer for fabricating nanoparticles (NP) due to its excellent biodegradability and biocompatibility, well-documented utility for sustained drug release, and approval by FDA for human use in a number of therapeutic devices (Kamaly et al., 2016). The development of PLGA NPs further enhances the efficacy of intracellular drug delivery to the adipocytes within specific subcutaneous WAT depots in pigs, allowing the encapsulated Notch inhibitor to sustain its pharmacological action over a prolonged period of time. These findings provide insights into the contribution of Notch inhibition in the metabolism of adipose tissue in a large animal model and highlight the therapeutic potential of targeting Notch signaling in obesity treatment.

RESULTS

DBZ Promotes Beige Adipogenesis and Mitochondrial Thermogenesis in Porcine Adipocytes through Inhibition of Notch Signaling *In Vitro*

To determine the role of Notch signaling in porcine adipogenesis, DBZ was used to inhibit γ-secretase that is essential for the activation of Notch signaling through mediating the cleavage of Notch intracellular domain (NICD). Preadipocytes isolated from subcutaneous fat of young pigs were treated with DBZ (10 μM) or vehicle control (DMSO, 0.1% v/v) after induced to differentiate. As shown in Figure 1A, differentiation of porcine adipocytes was efficiently induced with lipid droplets formed after incubation with induction medium for five days followed by differentiation medium for four days. Both phase contrast and oil red O staining images confirmed that the number of lipid droplets increased in the DBZ-treated cells compared with the vehicle control group, suggesting that the treatment with DBZ enhanced the differentiation efficiency of porcine preadipocytes. However, there were no obvious differences in the size of lipid droplets between two groups. Total lipid content within the cells was further measured by quantitative analysis of oil red O intensity. The results showed that the absorbance value of oil red O extracted from the DBZ-treated cells was 1.18-fold higher than that in the control group (Figure 1B, $p \leq 0.01$), demonstrating that DBZ promoted the differentiation of porcine preadipocytes and accumulation of lipid droplets.

We also examined the gene expression in DBZ and vehicle control treated porcine adipocytes using real-time qPCR. The mRNA expression of HES1, a Notch downstream target gene, was significantly inhibited after the DBZ treatment ($p \leq 0.05$), suggesting efficient inhibition of Notch signaling. Importantly, the expression of adipogenic and beige-fat-selective genes, including fatty acid binding protein 4 (FABP4, $p \leq 0.05$), peroxisome-proliferator-activated receptor gamma coactivator 1-alpha (PGC1α, $p \leq 0.05$), and cell-death-inducing DNA fragmentation factor alpha-like effector A (CIDEA, $p \leq 0.01$), were all significantly upregulated in the DBZ-treated cells (Figure 1C). The cells treated with DBZ also expressed a higher mRNA level of type 2 deiodinase (DIO2) than the control; however, the difference was not statistically significant ($p > 0.05$). The differentiation and gene expression results together indicate that the DBZ treatment promotes beige adipogenesis through efficient inhibition of Notch signaling pathway.

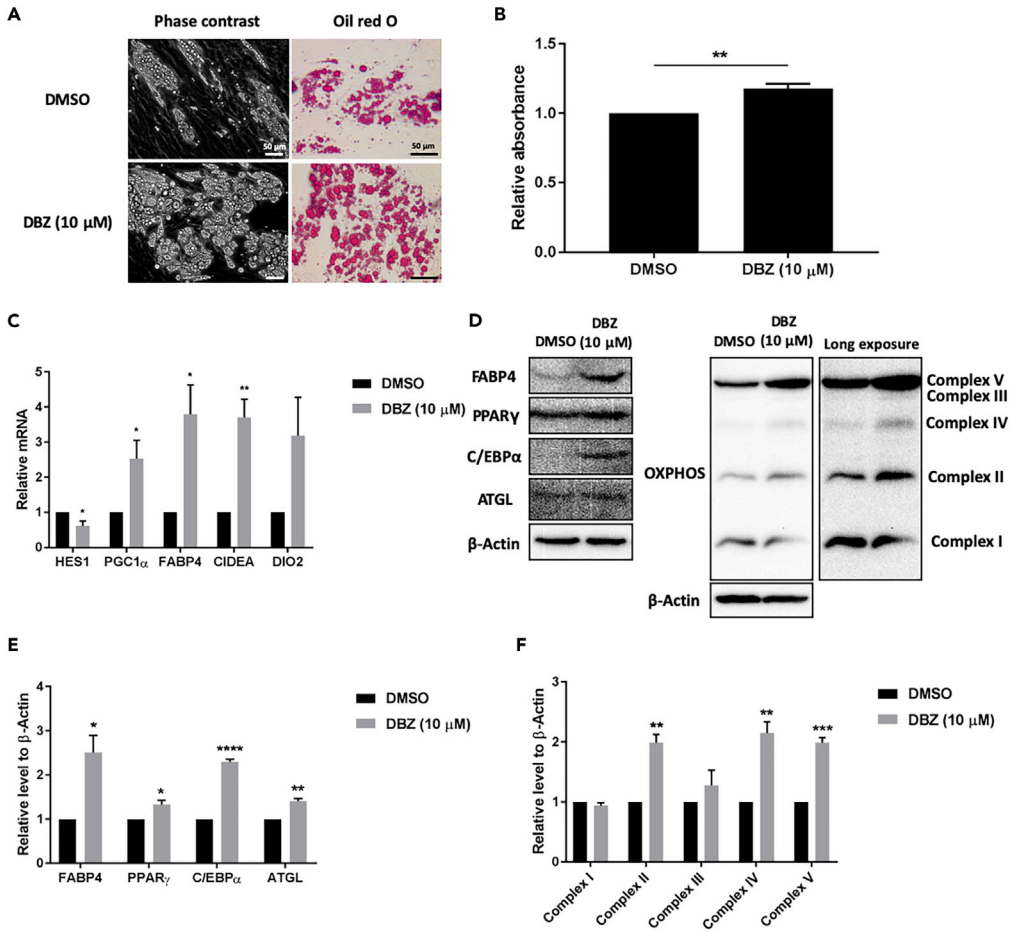

Figure 1. DBZ Promotes Beige Adipogenesis and Mitochondrial Thermogenesis in Porcine Adipocytes through Inhibition of Notch Signaling *In Vitro*

(A) Phase contrast and bright field images of differentiated porcine adipocytes stained with oil red O.

(B) Relative absorbance of oil red O extracted from stained porcine adipocytes.

(C) Real-time qPCR analysis showing the mRNA levels of Notch target (HES1), adipogenic (FABP4 and PGC1α), and beige-fat-selective genes (CIDEA and DIO2).

(D) Western blot results showing the protein expression levels of adipogenic (FABP4, PPARγ, and C/EBPα) and lipolytic (ATGL) markers as well as mitochondrial OXPHOS in differentiated porcine adipocytes treated with DBZ.

(E and F) Quantification of protein expression levels of adipogenic (FABP4, PPARγ, and C/EBPα) and lipolytic (ATGL) markers (E) and mitochondrial OXPHOS (F) normalized to β-Actin controls by densitometry analysis.

Consistently, Western blot analysis revealed that the protein expression levels of adipogenic genes, including CCAAT/enhancer-binding protein alpha (C/EBPα, $p \leq 0.001$), FABP4 ($p \leq 0.05$), and peroxisome-proliferator-activated receptor gamma (PPARγ, $p \leq 0.05$) significantly increased after the DBZ treatment (Figures 1D and 1E). Moreover, the DBZ-treated cells exhibited upregulated protein expression of adipose triglyceride lipase (ATGL, $p \leq 0.01$), which is a well-recognized lipolysis rate-limiting enzyme in adipocytes (Figures 1D and 1E). Adipocyte lipolysis is generally mediated by a complicated process that involves a number of lipases and proteins associated with lipid droplets. Our data suggest that the treatment with DBZ promotes beige adipogenesis and lipolysis synergistically. Furthermore, enhanced protein expression of oxidative phosphorylation (OXPHOS) was also observed in the DBZ group compared with the control, particularly for the complexes II ($p \leq 0.01$), IV ($p \leq 0.01$), and V ($p \leq 0.005$) (Figures 1D and 1F). These results demonstrate a potential intrinsic association of recruitment of beige adipocytes with mitochondrial biogenesis and oxidative capacity.

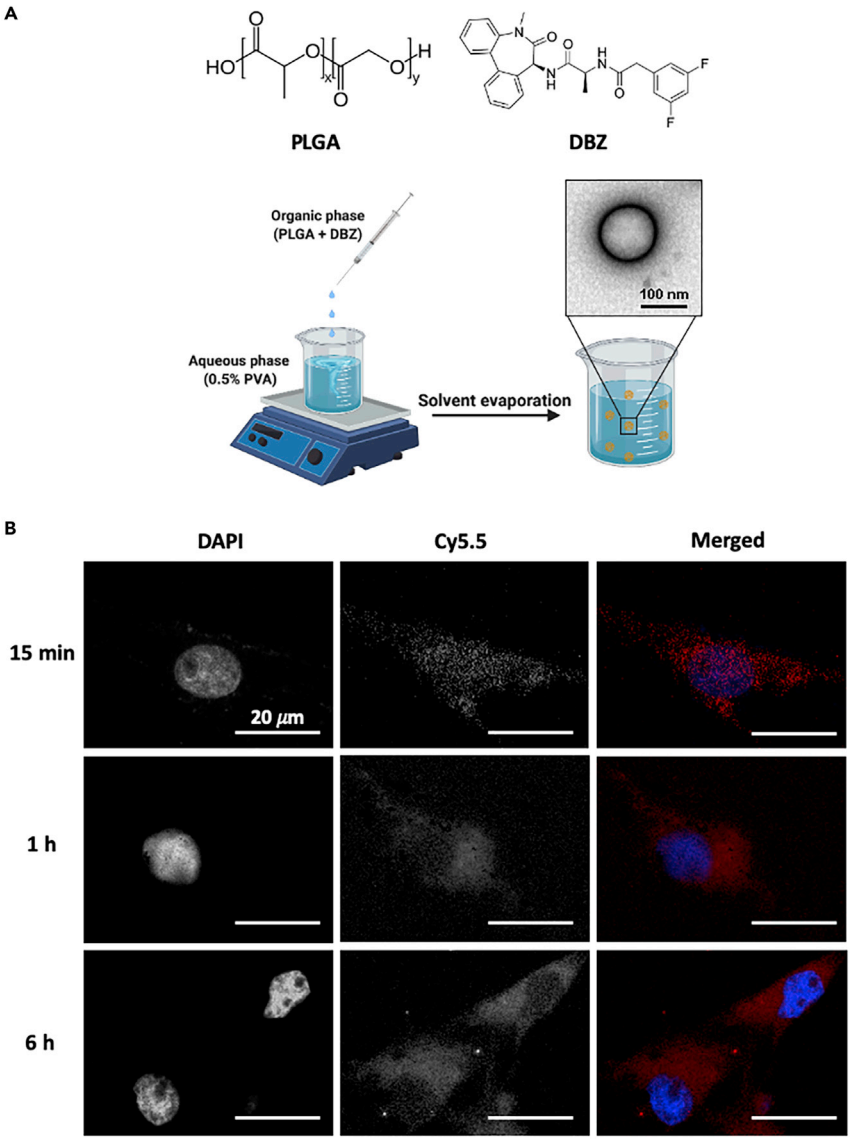

Figure 2. PLGA NPs Enable Rapid Cellular Uptake in Porcine Preadipocytes

(A) DBZ-encapsulated NPs prepared by the nanoprecipitation technique showing a spherical shape with a particle size ranging from 100 nm to 200 nm.

(B) *In vitro* cellular uptake of Cy5.5-conjugated NPs in primary porcine preadipocytes after 15 min, 1 h, and 6 h of incubation.

PLGA NPs Enable Rapid Cellular Uptake in Porcine Preadipocytes

To leverage benefits of polymeric NPs to achieve sustained intracellular drug release, we prepared PLGA NPs using the nanoprecipitation technique (Figure 2A). The NPs possessed an average particle size of 177 $\pm$ 6 nm and a negative surface charge with zeta potential of -20.2 ± 3.0 mV. A high encapsulation efficiency of 94% and sustained drug release for over one week *in vitro* were achieved with optimized parameters (Jiang et al., 2017). The morphology of NPs was visualized using transmission electron microscopy (TEM). NPs demonstrated a spherical shape with a particle size ranging from 100 nm to 200 nm, which was consistent with the result obtained by dynamic scattering light (Figure 2A). Cellular internalization of NPs was examined by incubating porcine preadipocytes with fluorescent dye Cy5.5-conjugated NPs for different periods of time (i.e. 15 min, 1 h, and 6 h). As shown in Figure 2B, a punctate and well-dispersed red fluorescent signal originating from Cy5.5-conjugated NPs was detected inside the cells, indicating

that NPs have been rapidly taken up by porcine preadipocytes within 15 min. Endocytosis could be the principal mechanism contributing to the superior cellular internalization efficiency of NPs (Jiang et al., 2017). When the incubation time of NPs was extended to 1 h, NPs were found to be distributed throughout the entire cytoplasm with a more homogeneous pattern compared with the early time point, which demonstrates the escape of NPs from endocytic vesicles. After 6 h of incubation, the red fluorescent signal in cells remained detectable, but the intensity and distribution pattern were similar to that observed at the 1 h time point, suggesting that cellular uptake of NPs in porcine preadipocytes was saturated within 1 h of incubation period. Our results reveal that NPs can be quickly taken up by primary porcine preadipocytes within 15 min and retained inside the cells for a prolonged period of time. Therefore, NP-mediated drug delivery can potentially reduce the frequency of administration and allow the encapsulated drug to sustain its pharmacological action.

DBZ-Loaded NPs Inhibit Notch Signaling, Promote Beige Adipogenesis and Mitochondrial Biogenesis in Porcine Adipocytes *In Vitro*

Primary porcine preadipocytes were treated with DBZ-encapsulated NPs at a final NP concentration of 0.1 mg/mL on the first and fifth days of differentiation. As shown in Figure 3A, more lipid droplets were embedded and accumulated in the cytoplasm of adipocytes treated with DBZ-loaded NPs than the control group treated with blank NPs, suggesting that DBZ enhances the differentiation efficiency of porcine preadipocytes. Total lipid content within the cells was also quantified by measuring the absorbance of oil red O extracted from stained adipocytes. The absorbance value in the group treated with DBZ-encapsulated NPs was 1.58-fold higher than that in the blank NP group (Figure 3B, $p \leq 0.005$). This finding indicates that efficient intracellular delivery and release of DBZ are achieved through rapid cellular internalization of NPs to promote the differentiation of porcine preadipocytes and accumulation of lipid droplets. It was also noted that the enhancement of cell differentiation achieved by the short-time incubation of DBZ-encapsulated NPs (i.e. 1.58-fold increase) was more robust than the treatment with native DBZ (i.e. 1.18-fold increase) at comparable drug concentrations. These results demonstrate that encapsulation of hydrophobic DBZ into NPs enables controlled drug delivery and target the agent toward the cells of interest, thereby improving its bioavailability and therapeutic efficacy.

Figure 3C illustrates the changes in mRNA expression of Notch target, adipogenic, and beige-fat-selective genes in differentiated adipocytes following the treatment with DBZ-loaded NPs. The treatment with DBZ-encapsulated NPs significantly inhibited the mRNA expression of HES1 ($p \leq 0.01$), whereas increased the mRNA expression of adipogenic and beige-fat-selective genes, including FABP4 ($p \leq 0.05$), PPARγ ($p \leq 0.05$), PGC1α ($p \leq 0.005$), CIDEA ($p \leq 0.05$), and DIO2 ($p \leq 0.01$), which was consistent with the results shown in Figure 1C. Moreover, the mRNA expression levels of mitochondria-related genes, such as cytochrome c oxidase (COX) 1 and 5B, were also upregulated after the treatment of DBZ-loaded NPs compared with the control group. Particularly, the change in COX1 expression was statistically significant ($p \leq 0.05$). Previous studies have shown that stimulation of COX activity is a key initiator for the recruitment of beige adipocytes (Madsen et al., 2010). COX produces prostaglandins or related products that promote mitochondrial biogenesis and increase the uncoupling capacity upon activation by norepinephrine or cold acclimatization (Barbatelli et al., 2010). Overall, these results indicate that the released DBZ from NPs maintains its biological activity to promote beige adipogenesis and mitochondrial oxidative metabolism through efficient and sustained inhibition of Notch signaling pathway.

The changes in protein expression were analyzed by western blotting with results shown in Figures 3D and 3E. Similar to the result of native DBZ treatment, the protein levels of adipogenic genes, including FABP4 ($p \leq 0.005$), PPARγ ($p \leq 0.005$), and C/EBPα ($p \leq 0.05$), significantly increased after the treatment with DBZ-loaded NPs. The expression of ATGL was also investigated to determine whether inhibition of Notch signaling was involved in regulation of other lipid metabolism activities, such as lipolysis that provides fuel for thermogenesis (Schreiber et al., 2017). The differentiated porcine adipocytes treated with DBZ-loaded NPs exhibited an upregulated protein expression level of ATGL compared with that in the control group ($p \leq 0.05$), indicating promoted lipolytic activities of porcine adipocytes. Taken together, our results demonstrate that DBZ-encapsulated NPs are quickly taken up by primacy porcine preadipocytes within 1 h and retained inside the cells to achieve efficient and sustained inhibition of Notch signaling pathway, thereby promoting beige adipogenesis, mitochondrial biogenesis, and lipolysis for an extended period of time.

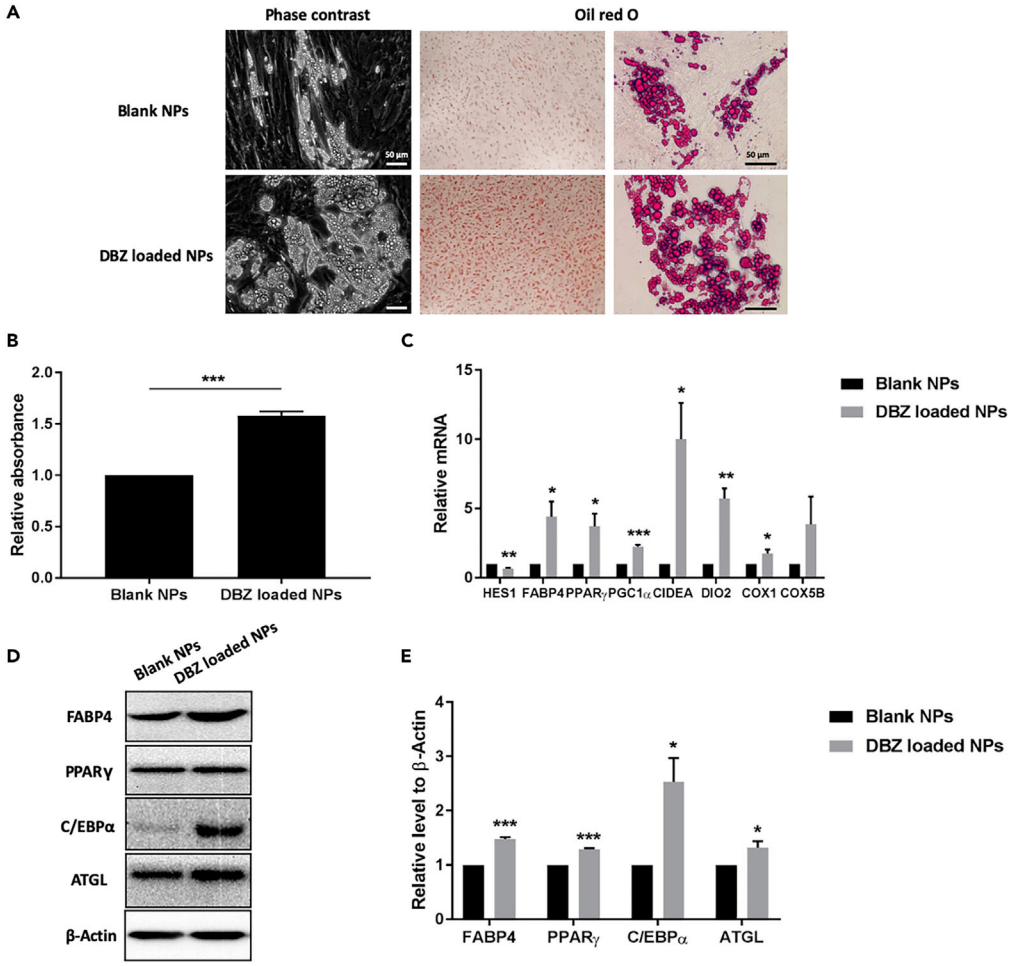

Figure 3. DBZ-Loaded NPs Inhibit Notch Signaling, Promote Beige Adipogenesis, and Mitochondrial Biogenesis in Porcine Adipocytes *In Vitro*

(A) Phase contrast and bright field images of differentiated porcine adipocytes stained with oil red O.

(B) Relative absorbance of oil red O extracted from stained adipocytes.

(C) Real-time qPCR analysis showing the mRNA levels of Notch target (HES1), adipogenic (FABP4, PPARγ, and PGC1α), beige-fat-selective genes (CIDEA and DIO2), and mitochondrial marker genes (COX1 and COX5B).

(D) Western blot results showing the protein expression levels of adipogenic (FABP4, PPARγ, and C/EBPα) and lipolytic (ATGL) marker genes in differentiated porcine adipocytes treated with DBZ loaded NPs.

(E) Quantification of protein expression levels of adipogenic (FABP4, PPARγ, and C/EBPα) and lipolytic (ATGL) markers normalized to β-Actin controls by densitometry analysis.

Local Injection of DBZ-Loaded NPs Increases the Number of Mitochondria and Multilocular Lipid Droplets in WAT in Pigs

To investigate the effect of NP-mediated Notch inhibition on recruitment of beige adipocytes in pigs *in vivo*, we injected blank or DBZ-encapsulated NPs into dorsal subcutaneous WAT of piglets (Figure 4B). WAT at the injection site was harvested from the pigs after five consecutive weekly administration of NPs (Figure 4A) and subjected to hematoxylin and eosin (H&E) staining as well as electron microscopy analysis. H&E staining revealed the morphological changes of adipocytes in the WAT depot in pigs (Figure 4C). WAT in the pigs receiving local injections of DBZ-loaded NPs exhibited a "brown-like" pattern with multilocular lipid droplets and shrinkage of adipocytes, demonstrating recruitment of beige adipocytes. Quantitative analysis of WAT depots also showed significant differences in adipocyte size distribution with an increase in the percentage of small adipocytes (<500 μm^2) and a reduction of large adipocyte population ($\geq$1000 μm^2) (Figure 4D). Consistently, both TEM (Figure 4E) and scanning electron microscopy (SEM) (Figure 4F) analysis confirmed that the number of mitochondria and beige adipocytes showing multilocular

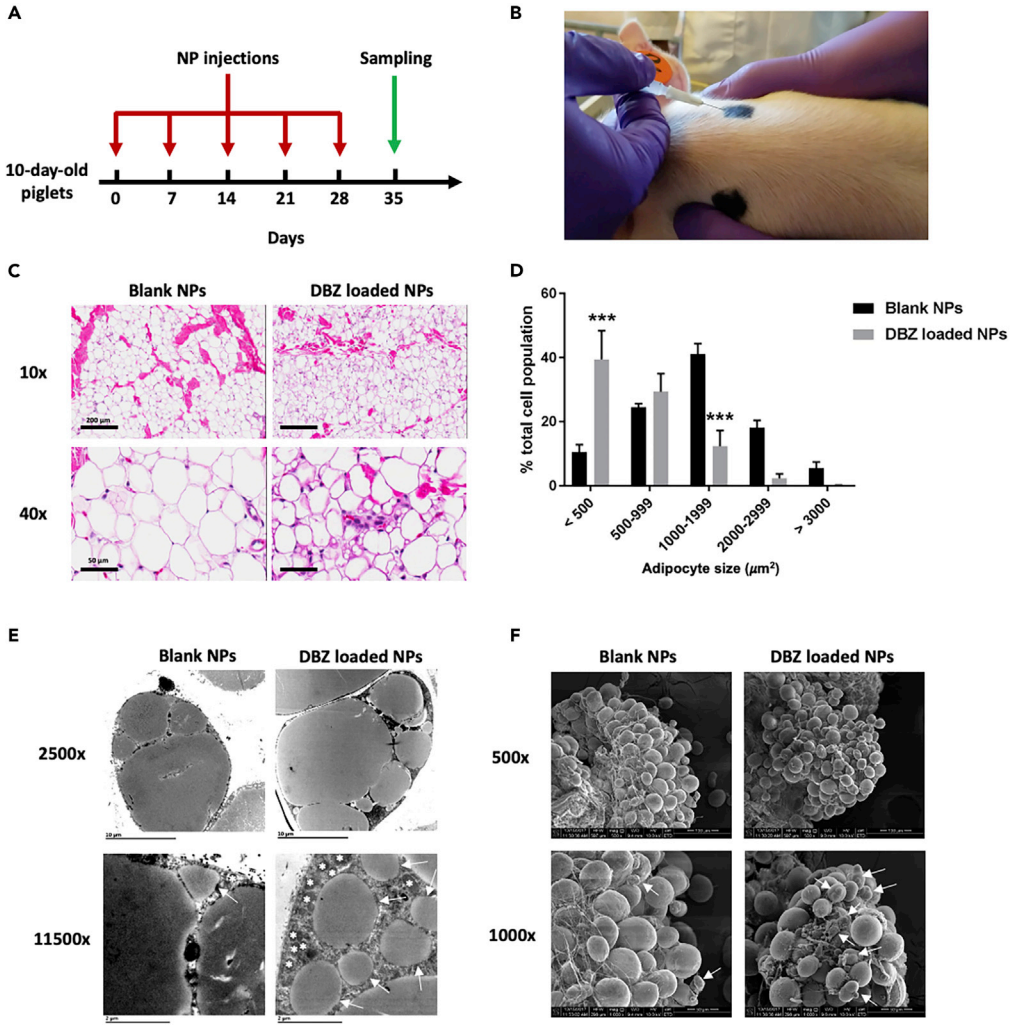

Figure 4. Local Injection of DBZ-Loaded NPs Increases the Number of Mitochondria and Multilocular Lipid Droplets in WAT in Pigs

(A) Experimental design showing the timeline of NP treatment in piglets.

(B) Picture showing the injection site on the shoulder of piglets.

(C) Representative images of H&E staining of WAT collected from the pigs after the treatment with blank or DBZ-loaded NPs.

(D) Quantitative size analysis of WAT adipocytes from the pigs treated with blank or DBZ-loaded NPs; 700–800 adipocytes in total from three pigs were analyzed for each group.

(E and F) Representative TEM (E) and SEM (F) images of porcine WAT after the treatment with blank or DBZ-loaded NPs. White asterisks and arrows mark mitochondria and multilocular lipid droplets in adipocytes, respectively.

droplet structures increased in WAT collected from the pigs injected with DBZ-encapsulated NPs compared with that in the blank-NP-treated pigs. WAT injected with DBZ-loaded NPs also contained a number of small lipid droplets, whereas the size of lipid droplets in WAT injected with blank NPs was relatively large and homogeneous. The presence of small lipid droplets indicate that adipocyte lipolysis might be enhanced in the local WAT depot following the treatment with DBZ-encapsulated NPs.

DISCUSSION

The Notch signaling pathway plays an important role in cell-cell communication and cell-fate determination during development. It is required for cellular homeostasis in virtually every metabolic organ, including skeletal muscle and adipose tissue (Bi and Kuang, 2015). Our previous studies have discovered that Notch

signaling regulates browning of WAT in mice (Bi et al., 2014). However, it remains unknown whether the metabolic benefits of Notch inhibition are dependent on UCP1 and evolutionarily relevant in other mammalian species, particularly large animals. This present work reveals a previously unrecognized role of Notch signaling in the regulatory control of beige fat in pigs, a species that lacks a functional UCP1 protein due to deletion of exons 3–5 in the UCP1 gene (Berg et al., 2006). Molecular, cellular, and histological evidence were provided to demonstrate that pharmacological inhibition of Notch signaling promotes beige adipogenesis and mitochondrial biogenesis as well as reduces adiposity in WAT in pigs. Because Notch signaling is a highly conserved pathway in mammals, it is anticipated that these findings in mice and pigs will be applicable to humans, although further studies investigating the role of Notch signaling in human adipose tissue and its impact on obesity treatment are necessary.

We found that the treatment with a γ-secretase inhibitor DBZ promoted differentiation of porcine preadipocytes *in vitro*. DBZ at a concentration of 10 μM significantly inhibited mRNA expression of HES1 and upregulated adipogenic markers at both transcription and expression levels. The treatment also resulted in increased expression of lipolytic and beige-fat-selective genes. Generally, free fatty acids produced by lipolysis are catalyzed to form acetyl coenzyme A, which enters the mitochondria to participate in β-oxidation and generate heat (Ellis et al., 2010). This is the major pathway for the degradation of fatty acids and is associated with mitochondrial content and respiratory capability (Deveaud et al., 2004). These observations suggest Notch inhibition promotes beige adipogenesis, lipolysis, and mitochondrial biogenesis in porcine white adipocytes. The Delta-like and Serrate/Jagged family of membrane bound ligands bind to transmembrane Notch receptors, which induces γ-secretase-mediated proteolytic cleavage of Notch and subsequently results in the nuclear translocation of NICD. Once NICD is located in the nucleus, it activates the recombination signal-binding protein for immunoglobulin kappa J region transcriptional complex along with its downstream targets, such as the HES family genes (Schroeter et al., 1998). Our previous results have shown that the Notch signaling plays a critical role in regulation of adipose browning with pharmacological inhibition of Notch signaling promoting beige adipogenesis and ameliorating obesity in obese mice (Bi et al., 2014). The underlying mechanism is that the Notch downstream target gene HES1 directly binds to the promoter regions of PR-domain-containing 16 (PRDM16) and PGC1α to repress their transcription. These two genes have previously been identified as master regulators of beige adipogenesis and mitochondrial biogenesis (Austin and St-Pierre, 2012) (Seale et al., 2007). Because the Notch signaling is a highly conserved pathway, it is believed that its functions in regulation of metabolism could be potentially extended to large animals.

UCP1 has long been considered the key thermogenic protein mediating non-shivering thermogenesis and playing a crucial role in regulation of adipose conversion (Nedergaard et al., 2001) (Shabalina et al., 2013). However, some studies in transgenic rodent models show unexpected results with regard to the metabolic phenotypes between beige-adipocyte-deficient and UCP1-deficient mice. Specifically, beige-adipocyte-deficient mice induced by the adipocyte-specific deletion of PRDM16 developed obesity even under ambient temperature conditions, whereas UCP1 knockout mice displayed obese phenotypes only when they were kept at thermoneutrality (Cohen et al., 2014) (Feldmann et al., 2009). The difference in metabolic phenotypes between these mouse models therefore implies the existence of UCP1-independent thermogenic mechanisms. More recently, calcium cycling has been determined to regulate beige thermogenesis independently of UCP1 (Ikeda et al., 2017). Creatine-based futile cycle was also found to be an important mechanism of thermoregulation, independent of UCP1 (Kazak et al., 2015). The discovery of UCP1-independent thermogenic mechanisms may open up possibilities for improvement of metabolic health, particularly in the elderly who do not possess UCP1-positively expressed adipocytes. In this present work, the role of Notch signaling pathway in regulation of beige fat recruitment was investigated in the pig, which is a unique animal model for obesity research due to the lack of functional UCP1 protein and similarities of metabolic features to humans (Spurlock and Gabler, 2008) (Jastroch and Andersson, 2015). Our results confirm that inhibition of Notch signaling promotes the differentiation, beige adipogenesis, and mitochondrial biogenesis in porcine adipocytes despite their lack of the UCP1 protein.

Despite great potential of pharmacological inhibition shown in regulation of beige thermogenesis, translation of this therapeutic strategy for obesity treatment in the clinical settings could be hindered by the potential risks of off-target consequences, lack of control over the location, and acute toxicity induced by high dosage. Frequent injections aiming to maintain the effective therapeutic concentration also might result in unwanted side effects and patient compliance issue. Over the past decades, the field of nanomedicine has evolved alongside the

increasing technical needs to enhance the delivery efficiency of various therapeutics, including anti-obesity drugs (Huang et al., 2019). NP delivery systems offer both temporal and spatial control of drug release. There are a number of considerations when developing these NP formulations. For instance, cellular uptake, transport, and fate of NPs are strongly dependent on their physicochemical properties (Zhu et al., 2013). Acquirement of well-ordered and dispersed NPs with a highly predictable and desirable size as well as surface characteristics is therefore critical to achieve efficient intracellular delivery of NPs. In our studies, the small particle size and negative surface charge of NPs produced by an optimized nanoprecipitation process could facilitate diffusive mobility and strong repulsive interaction between particles, thus preventing agglomeration and stabilizing NP dispersions. The optimized NPs exhibited rapid cellular internalization in porcine preadipocytes through endocytotic trafficking followed by an endo-lysosome escape to the cytosol, allowing for prolonged intracellular retention and sustained DBZ release for over one week under the physiological condition (Jiang et al., 2017). Sustained release NP formulations can also help improve patient compliance by minimizing dose frequency. For effective treatment of chronic diseases, such as obesity, a prolonged release behavior can maintain the therapeutic dose for longer periods of time, minimizing both underexposure and the risk of toxicity from overexposure (Kamaly et al., 2016). In this work, the encapsulated DBZ was gradually transported out of NPs via diffusion or released from the polymer matrix upon degradation after taken up by porcine preadipocytes. The slowly released DBZ well maintained its bioactivity to achieve sustained inhibition of Notch signaling pathway during preadipocyte differentiation, as evidenced by the efficient downregulation of Notch target gene and resultant elevation of adipogenic, lipolytic, beige-fat-selective, and mitochondrial gene expression. More importantly, direct injection of DBZ-encapsulated NPs into the subcutaneous WAT depots in pigs resulted in efficient and site-specific delivery of Notch inhibitors. The WAT injected with DBZ-loaded NPs exhibited considerable morphological changes with an increased number of mitochondria and multilocular lipid droplets. Local injection into the target tissue is a promising approach to achieve site specificity, permit a reduction in dosage, and avoid drug diffusion to the other off-target organs (Huang et al., 2019) (Jiang et al., 2015) (Jiang et al., 2017). In addition, slowly released drugs from NPs could allow sustained inhibition of Notch signaling over an extended period of time, thereby improving the therapeutic efficacy and reducing the need for frequent injections as well as potential risks of side effects. These *in vivo* observations are consistent with our *in vitro* results, demonstrating that both recruitment of beige adipocytes and mitochondrial biogenesis in WAT in pigs are promoted by inhibition of Notch signaling through efficient intracellular delivery of DBZ-loaded NPs.

Overall, we have shown that pharmacological inhibition of Notch signaling pathway through administration of DBZ promotes beige adipogenesis and mitochondrial biogenesis in adipocytes of pigs, which lack of functional UCP1 protein. Encapsulation of DBZ into a synthetic PLGA-based nanoparticulate delivery system enables rapid cellular internalization and controlled drug delivery in adipocytes to achieve efficient and sustained Notch inhibition, thereby promoting beige adipogenesis, thermogenesis, and lipolysis *in vitro*. More importantly, injection of DBZ-encapsulated NPs into the subcutaneous WAT depot in pigs leads to localized NP delivery, inducing increased mitochondrial numbers and reduced subcutaneous adipose tissue expansion *in vivo*. This study demonstrates for the first time that Notch signaling is a negative regulator of beige adipocyte biogenesis in a large animal model, highlighting the therapeutic potential of targeting Notch signaling in obesity treatment.

Limitations of the Study

We have shown that inhibition of Notch signaling pathway promotes beige adipogenesis and mitochondrial biogenesis in pigs that lack functional UCP1 protein. However, the detailed molecular mechanism by which Notch signaling regulates beige thermogenesis remains unknown and is a subject for future research.

Resource Availability

Lead Contact

Further information and requests for resources and reagents should be directed to and will be fulfilled by the lead contact, Meng Deng (deng65@purdue.edu).

Materials Availability

All unique/stable reagents generated in this study will be made available on request, but we may require a payment and/or a completed Materials Transfer Agreement if there is potential for commercial application.

Data and Code Availability

The original/source data are available from the lead contact on request.

METHODS

All methods can be found in the accompanying Transparent Methods supplemental file.

SUPPLEMENTAL INFORMATION

Supplemental Information can be found online at https://doi.org/10.1016/j.isci.2020.101167.

ACKNOWLEDGMENTS

The authors appreciate the funding support from the National Institute of Diabetes and Digestive and Kidney Diseases (R43DK115277 to M. D.), National Cancer Institute (R01CA212609 to S. K.), and AgSEED (Purdue University's competitive internal grant program: Agricultural Science and Extension for Economic Development, to S. K., M. D., and K. M. A.).

AUTHOR CONTRIBUTIONS

S. K. and M. D. conceptualized and supervised the study; D. H. designed and conducted the *in vitro* experiments; N. N., M. A. C.-V., Z. J., and K. M. A. designed and conducted the *in vivo* experiments; K. M. A. provided the primary porcine preadipocytes; D. H. wrote the original draft; S. K. and M. D. reviewed and edited the manuscript.

DECLARATION OF INTERESTS

M. D. and S. K. are co-inventors on a patent application entitled "Polymer-based Therapeutics for Inductive Browning of Fat" (International PCT Patent Application Number: PCT/US16/58997) and disclose financial interest in Adipo Therapeutics, a university startup developing polymer technologies for applications in adipocytes.

Received: March 5, 2020
Revised: April 1, 2020
Accepted: May 11, 2020
Published: June 26, 2020

REFERENCES

Austin, S., and St-Pierre, J. (2012). PGC1α and mitochondrial metabolism - emerging concepts and relevance in ageing and neurodegenerative disorders. J. Cell Sci. *125*, 4963–4971.

Barbatelli, G., Murano, I., Madsen, L., Hao, Q., Jimenez, M., Kristiansen, K., Giacobino, J.P., De Matteis, R., and Cinti, S. (2010). The emergence of cold-induced brown adipocytes in mouse white fat depots is determined predominantly by white to brown adipocyte transdifferentiation. Am. J. Physiol. Endocrinol. Metab. *298*, E1244–E1253.

Berg, F., Gustafson, U., and Andersson, L. (2006). The uncoupling protein 1 gene (UCP1) is disrupted in the pig lineage: a genetic explanation for poor thermoregulation in piglets. PLoS Genet. *2*, 1178–1181.

Bi, P., and Kuang, S. (2015). Notch signaling as a novel regulator of metabolism. Trends Endocrinol. Metab. *26*, 248–255.

Bi, P., Shan, T., Liu, W., Yue, F., Yang, X., Liang, X.R., Wang, J., Li, J., Carlesso, N., Liu, X., and Kuang, S. (2014). Inhibition of Notch signaling promotes browning of white adipose tissue and ameliorates obesity. Nat. Med. *20*, 911–918.

Cohen, P., Levy, J.D., Zhang, Y., Frontini, A., Kolodin, D.P., Svensson, K.J., Lo, J.C., Zeng, X., Ye, L., Khandekar, M.J., et al. (2014). Ablation of PRDM16 and beige adipose causes metabolic dysfunction and a subcutaneous to visceral fat switch. Cell *156*, 304–316.

Deveaud, C., Beauvoit, B., Salin, B., Schaeffer, J., and Rigoulet, M. (2004). Regional differences in oxidative capacity of rat white adipose tissue are linked to the mitochondrial content of mature adipocytes. Mol. Cell. Biochem. *267*, 157–166.

Ellis, J.M., Li, L.O., Wu, P.C., Koves, T.R., Ilkayeva, O., Stevens, R.D., Watkins, S.M., Muoio, D.M., and Coleman, R.A. (2010). Adipose Acyl-CoA synthetase-1 directs fatty acids toward β-oxidation and is required for cold thermogenesis. Cell Metab. *12*, 53–64.

Feldmann, H.M., Golozoubova, V., Cannon, B., and Nedergaard, J. (2009). UCP1 ablation induces obesity and abolishes diet-induced thermogenesis in mice exempt from thermal stress by living at thermoneutrality. Cell Metab. *9*, 203–209.

Huang, D., Deng, M., and Kuang, S. (2019). Polymeric carriers for controlled drug delivery in obesity treatment. Trends Endocrinol. Metab. *30*, 974–989.

Ikeda, K., Kang, Q., Yoneshiro, T., Camporez, J.P., Maki, H., Homma, M., Shinoda, K., Chen, Y., Lu, X., Maretich, P., et al. (2017). UCP1-independent signaling involving SERCA2bmediated calcium cycling regulates beige fat thermogenesis and systemic glucose homeostasis. Nat. Med. *23*, 1454–1465.

Jastroch, M., and Andersson, L. (2015). When pigs fly, UCP1 makes heat. Mol. Metab. *4*, 359–362.

Jiang, C., Cano-Vega, M.A., Yue, F., Kuang, L., Narayanan, N., Uzunalli, G., Merkel, M.P., Kuang, S., and Deng, M. (2017). Dibenzazepine-loaded nanoparticles induce local browning of white adipose tissue to counteract obesity. Mol. Ther. *25*, 1718–1729.

Jiang, C., Kuang, L., Merkel, M.P., Yue, F., Cano-Vega, M.A., Narayanan, N., Kuang, S., and Deng, M. (2015). Biodegradable polymeric microsphere-based drug delivery for inductive browning of fat. Front. Endocrinol. (Lausanne) *6*, 1–11.

Kajimura, S., and Saito, M. (2014). A new era in Brown adipose tissue biology: molecular control of Brown fat development and energy homeostasis. Annu. Rev. Physiol. *76*, 225–249.

Kamaly, N., Yameen, B., Wu, J., and Farokhzad, O.C. (2016). Degradable controlled-release polymers and polymeric nanoparticles: mechanisms of controlling drug release. Chem. Rev. *116*, 2602–2663.

Kazak, L., Chouchani, E.T., Jedrychowski, M.P., Erickson, B.K., Shinoda, K., Cohen, P., Vetrivelan, R., Lu, G.Z., Laznik-Bogoslavski, D., Hasenfuss, S.C., et al. (2015). A creatine-driven substrate cycle enhances energy expenditure and thermogenesis in beige fat. Cell *163*, 643–655.

Lidell, M.E., Betz, M.J., Leinhard, O.D., Heglind, M., Elander, L., Slawik, M., Mussack, T., Nilsson, D., Romu, T., Nuutila, P., et al. (2013). Evidence for two types of brown adipose tissue in humans. Nat. Med. *19*, 631–634.

Lshibashi, J., and Seale, P. (2010). Beige can be slimming. Science *328*, 1113–1114.

Madsen, L., Pedersen, L.M., Lillefosse, H.H., Fjære, E., Bronstad, I., Hao, Q., Petersen, R.K., Hallenborg, P., Ma, T., de Matteis, R., et al. (2010). UCP1 induction during recruitment of brown adipocytes in white adipose tissue is dependent on cyclooxygenase activity. PLoS One *5*, e11391.

Moisan, A., Lee, Y.K., Zhang, J.D., Hudak, C.S., Meyer, C.A., Prummer, M., Zoffmann, S., Truong, H.H., Ebeling, M., Kiialainen, A., et al. (2015). White-to-brown metabolic conversion of human adipocytes by JAK inhibition. Nat. Cell Biol. *17*, 57–67.

Nedergaard, J., Golozoubova, V., Matthias, A., Asadi, A., Jacobsson, A., and Cannon, B. (2001). UCP1: the only protein able to mediate adaptive non-shivering thermogenesis and metabolic inefficiency. Biochim. Biophys. Acta Bioenerg. *1504*, 82–106.

Ohno, H., Shinoda, K., Spiegelman, B.M., and Kajimura, S. (2012). PPARγ agonists induce a white-to-brown fat conversion through stabilization of PRDM16 protein. Cell Metab. *15*, 395–404.

Ost, M., Keipert, S., and Klaus, S. (2017). Targeted mitochondrial uncoupling beyond UCP1 – the fine line between death and metabolic health. Biochimie *134*, 77–85.

Petrovic, N., Walden, T.B., Shabalina, I.G., Timmons, J.A., Cannon, B., and Nedergaard, J. (2010). Chronic peroxisome proliferator-activated receptor γ (PPARγ) activation of epididymally derived white adipocyte cultures reveals a population of thermogenically competent, UCP1-containing adipocytes molecularly distinct from classic brown adipocytes. J. Biol. Chem. *285*, 7153–7164.

Pilitsi, E., Farr, O.M., Polyzos, S.A., Perakakis, N., Nolen-Doerr, E., Papathanasiou, A.E., and Mantzoros, C.S. (2018). Pharmacotherapy of obesity: available medications and drugs under investigation. Metabolism *92*, 170–192.

Rosen, E.D., and Spiegelman, B.M. (2006). Adipocytes as regulators of energy balance and glucose homeostasis. Nature *444*, 847–853.

Schreiber, R., Diwoky, C., Schoiswohl, G., Feiler, U., Wongsiriroj, N., Abdellatif, M., Kolb, D., Hoeks, J., Kershaw, E.E., Sedej, S., et al. (2017). Cold-induced thermogenesis depends on ATGL-mediated lipolysis in cardiac muscle, but not Brown adipose tissue. Cell Metab. *26*, 753–763.e7.

Schroeter, E.H., Kisslinger, J.A., and Kopan, R. (1998). Notch-1 signalling requires ligand-induced proteolytic release of intracellular domain. Nature *393*, 382–386.

Seale, P., Kajimura, S., Yang, W., Chin, S., Rohas, L.M., Uldry, M., Tavernier, G., Langin, D., and Spiegelman, B.M. (2007). Transcriptional control of Brown fat determination by PRDM16. Cell Metab. *6*, 38–54.

Shabalina, I.G., Petrovic, N., deJong, J.M.A., Kalinovich, A.V., Cannon, B., and Nedergaard, J. (2013). UCP1 in Brite/Beige adipose tissue mitochondria is functionally thermogenic. Cell Rep. *5*, 1196–1203.

Spurlock, M.E., and Gabler, N.K. (2008). The development of porcine models of obesity and the metabolic syndrome. J. Nutr. *138*, 397–402.

Wu, J., Boström, P., Sparks, L.M., Ye, L., Choi, J.H., Giang, A.H., Khandekar, M., Virtanen, K.A., Nuutila, P., Schaart, G., et al. (2012). Beige adipocytes are a distinct type of thermogenic fat cell in mouse and human. Cell *150*, 366–376.

Zheng, Q., Lin, J., Huang, J., Zhang, H., Zhang, R., Zhang, X., Cao, C., Hambly, C., Qin, G., Yao, J., et al. (2017). Reconstitution of UCP1 using CRISPR/Cas9 in the white adipose tissue of pigs decreases fat deposition and improves thermogenic capacity. Proc. Natl. Acad. Sci. U S A *114*, E9474–E9482.

Zhu, M., Nie, G., Meng, H., Xia, T., Nel, A., and Zhao, Y. (2013). Physicochemical properties determine nanomaterial cellular uptake, transport, and fate. Acc. Chem. Res. *46*, 622–631.

iScience, Volume *23*

Supplemental Information

Nanoparticle-Mediated Inhibition of Notch Signaling Promotes Mitochondrial Biogenesis and Reduces Subcutaneous Adipose Tissue Expansion in Pigs

Di Huang, Naagarajan Narayanan, Mario A. Cano-Vega, Zhihao Jia, Kolapo M. Ajuwon, Shihuan Kuang, and Meng Deng

Table S1. Primers used in the real-time qPCR analysis, related to Figures 1 and 3.

Gene	Sequence
HES1	5’-TTCTCCAGCTTGGAATGCCT-3’
	5’-ACACGACACCGGATAAACCAA-3’
PPARγ	5’-GGCTGCTATCATTTGGTGCG-3’
	5’-GCACGATACCCTCCTGCATT-3’
PGC1α	5’-TGTGCAACCAGGACTCTGTA-3’
	5’-CCACTTGAGTCCACCCAGAAA-3’
FABP4	5’-GAGCACCATAACCTTAGATGGA-3’
	5’-AAATTCTGGTAGCCGTGACA-3’
CIDEA	5’-TGCCATCTTCCTCCAACACTAA-3’
	5’-TTCCGAGTTTCCAACCACAA-3’
DIO2	5’-AGAGATGGGCAGAGGCAAAC-3’
	5’-GACGGAGATGTGCAGAGGTT-3’
COX1	5’-CAATGCCCGTTAGACCTCC-3’
	5’-ACCCGAGCATACTTTACATCTG-3’
COX5B	5’-CAGCCCACTATCCGCTTGTT-3’
	5’-TTGTGCGGTCTATGGCATCT-3’
β-Actin	5’-GGACTTCGAGCAGGAGATGG-3’
	5’-AGGAAGGAGGGCTGGAAGAG-3’

TRANSPARENT METHODS

Materials

PLGA (Inherent viscosity: 0.45-0.60 dL/g; Mw: 30,000 Da; 50:50 LA:GA (w:w)) was obtained from Boehringer Ingelheim (Ingelheim am Rhein, Germany). DBZ was purchased from Tocris Bioscience (Bristol, UK). PLGA with a terminal amine group (PLGA-NH_2, Mw: 30,000 Da) was purchased from PolySciTech (West Lafayette, IN, USA). The N-hydroxysuccinimidyl ester form of cyanine 5.5 (Cy5.5-NHS) was purchased from Click Chemistry Tools (Scottsdale, AZ, USA). FABP4 (SC-271529), C/EBPα (SC-61), and β-Actin (SC-47778) antibodies were purchased from Santa Cruz Biotechnology (Dallas, TX, USA). The OXPHO (S45-8099) antibody was obtained from Invitrogen (Carlsbad, CA, USA). PPARγ (81B8) and ATGL (30A4) antibodies as well as horseradish peroxidase (HRP)-conjugated secondary antibodies, including anti-rabbit immunoglobulin G (IgG) (7074S) and anti-mouse IgG (7076S), were purchased from Cell Signaling Technology (Danvers, MA, USA). Acetone was purchased from Fisher Scientific (Hampton, NH, USA). All other reagents and solvents were purchased from Sigma-Aldrich (St. Louis, MO, USA).

Animals

All animal procedures were approved by the Purdue University Animal Care and Use Committee. All the pigs (10-day-old) used in this study were obtained from and housed at Purdue University Swine Research Unit. Room temperature was maintained at 20 ± 2 °C with a 12 h lighting program. The body weight of pigs was 3.0 kg at the beginning of the study and 8.9 kg at the end. They consumed an average feed of 0.25 kg/day during the experiment. Pigs were given weekly injections of NPs (blank NPs or DBZ loaded NPs) into the subcutaneous WAT depot on each side of their shoulders for successive five weeks. The concentration of NPs was 1 mg/mL in a volume of 0.5 mL phosphate-buffered saline (PBS). The injection sites were marked to ensure the consistency. Pigs were euthanized by exsanguination after five weeks and WAT at the injection sites was collected for analysis.

Cell culture

Adipose stromal vascular fraction cells from the subcutaneous WAT of neonatal piglets were cultured in Dulbecco's modified Eagle medium (DMEM) supplemented with 20% fetal bovine serum (FBS) and 1% antibiotics (penicillin and streptomycin) at 37 °C, 5% CO_2, and 95% relative humidity. Beige adipocyte differentiation was induced by treating confluent preadipocytes with the adipogenic induction medium containing DMEM, 10% FBS, 0.5 mM isobutylmethylxanthine, 1 μM dexamethasone, 1.75 μM insulin, 1 μM rosiglitazone, 10 nM triiodothyronine, 125 nM indomethacin, 17 μM pantothenic acid, and 30 μM biotin. Five days after induction, medium was switched to the differentiation medium containing DMEM, 10% FBS, 850 nM insulin, and 10 nM triiodothyronine until adipocytes matured.

For the treatment with native compounds, cells were treated with DBZ at a final concentration of 10 μM during induction and differentiation. For NP treatment, cells were rinsed with PBS for three times and incubated with serum-free DMEM containing NPs (blank NPs or DBZ loaded NPs) at a final concentration of 0.1 mg/mL for 1 h. After removal of NP suspensions, cells were rinsed with PBS and subjected to the adipogenic induction medium. Cells were treated with NPs again on the fifth day with the same procedure described above before changing to the differentiation medium.

Preparation of NPs

NPs were prepared using the nanoprecipitation method described previously (Jiang et al., 2017). Briefly, 10 mg of PLGA was dissolved in acetone with or without 0.5 mg of DBZ. The organic phase was quickly injected into the aqueous phase containing 1% polyvinyl alcohol (PVA, 87%-90% hydrolyzed, Mw 30-70 kDa) through a syringe under stirring at speed of 600 rpm. The mixture solutions were stirred for 6 h at room temperature to allow solvent evaporation and the resulting NP fractions were purified by centrifugation at 13,000 rpm for 50 min at 4 °C (Centrifuges 5804 R, Eppendorf, Hamburg, Germany) and resuspended in deionized water or PBS.

Fluorescence conjugated NPs were also prepared to track cellular uptake dynamics of NPs in porcine preadipocytes. The conjugation of Cy5.5-NHS ester and PLGA-NH_2 was performed by mixing 1.2 mg of Cy5.5-NHS ester and 33 mg of PLGA-NH_2 in 3 mL of DMSO in a Schlenk flask under nitrogen and stirring overnight at room temperature in darkness. The synthesized polymers

were purified by the solvent/non-solvent technique. The reaction mixture was dropped into 40 mL of cold methanol and centrifuged at 8,000 rpm at 4°C for 30 min. The pellet was re-dissolved in DMSO, precipitated, and washed repeatedly. The final products were dried in the vacuum oven at room temperature for 24 h. Cy5.5 conjugated NPs were prepared following the standard protocol described above.

Cellular uptake of NPs

Primary porcine SVF cells were seeded onto 12-well plates at a density of 1×10^5 cells per well and cultured for 48 h. After washing with PBS, cells were incubated with serum-free DMEM containing Cy5.5 conjugated NPs at a final concentration of 0.1 mg/mL for 15 min, 1 h, and 6 h. Subsequently, cells were washed three times with cold PBS to remove remaining NPs and dead cells. For fixed cell imaging, cells were treated with 300 μL of 4% paraformaldehyde (PFA) aqueous solution for 15 min followed by nuclear counterstain with 4′,6-diamidino-2-phenylindole (DAPI, 1 μg/mL in PBS) for 10 min at room temperature. Fluorescent images were captured using a CoolSnap HQ charge coupled-device camera (Photometrics, Tucson, AZ, USA) equipped on a Leica DM 6000B microscope (Leica Camera, Wetzlar, Germany) with a × 20 objective.

Morphological observation of lipid droplets

The morphology of mature adipocytes after treatments was observed using a Leica DM 6000B microscope (Leica Camera, Wetzlar, Germany) with a × 20 objective. Oil red O staining was subsequently conducted to demonstrate the presence of accumulated lipid droplets in the cells. Briefly, cells were fixed with 4% PFA and stained with freshly prepared oil red O working solutions containing 6 mL of oil red O stock stain (5 mg/mL in isopropanol) and 4 mL of ddH_2O for 15 min. The stained cells were washed repeatedly with PBS and photographed using a Nikon D90 digital camera installed on a Leica DM 6000B microscope with a × 20 objective. After imaging, oil red O was extracted from stained cells using isopropanol and absorbance was determined spectrophotometrically at a wavelength of 500 nm.

RNA extraction, cDNA synthesis, and real-time qPCR

Total RNA was extracted from cells using TRIzol (Thermo Fisher Scientific, Waltham, MA, USA) in accordance with the manufacturer's protocol. RNA was treated with RNase-free DNase I to

remove contaminating genomic DNA and the purity as well as concentration of extracted RNA were determined by a spectrophotometer NanoDrop 2000c (Thermo Fisher Scientific, Waltham, MA, USA). Subsequently, 2 μg of RNA was reverse transcribed to cDNA using random hexamer primers with M-MLV reverse transcriptase (Invitrogen, Carlsbad, CA, USA). Real-time qPCR was performed in the Roche Light Cycler 480 PCR system (Roche, Basel, Switzerland) with SYBR Green master mix. The sequences of gene-specific primers were listed in **Table S1**. The $2^{-\Delta\Delta CT}$ method was used to analyze the relative changes of gene expression after normalization to the expression of β-Actin.

Protein extraction and western blotting

Total protein was extracted from cells using RIPA buffer containing 25 mM Tris-HCl (pH 8.0), 150 mM NaCl, 1 mM EDTA, 0.5% NP-40, 0.5% sodium deoxycholate and 0.1% SDS. Protein concentrations were determined by Pierce BCA Protein Assay Reagent (Pierce Biotechnology, Waltham, MA, USA). Proteins were separated by SDS-PAGE and transferred to a polyvinylidene fluoride membrane (Millipore, Burlington, MA, USA). The membrane was then blocked with 5% fat-free milk for 1 h at room temperature and incubated with primary antibodies in 5% milk overnight at 4°C as well as secondary antibodies for 1 h at room temperature. Primary antibodies, including C/EBPα (1:500 dilution), FABP4 (1:500 dilution), PPARγ (1:500 dilution), OXPHOS (1:2000 dilution), and β-Actin (1:5000 dilution), were used. HRP-conjugated secondary antibodies, including anti-rabbit and anti-mouse IgG, were also used at a dilution of 1:10,000. A luminol reagent for enhanced chemiluminescence detection of western blots (Santa Cruz Biotechnology, Dallas, TX, USA) was employed and signals were detected with a FluorChem R imaging system (ProteinSimple, San Jose, CA, USA).

Histology

WAT collected from NP injected pigs was fixed in 10% formalin for 24 h at room temperature, embedded into paraffin, and cut into sections at a thickness of 5 μm. Slides were deparaffinized and incubated with xylene, ethanol, and deionized water sequentially for rehydration according to a standard protocol. For H&E staining, tissue sections were firstly stained with hematoxylin for 12 min, rinsed with running tap water for 2 min, and stained with eosin for 30 s. After staining, slides were dehydrated in graded ethanol (75%, 90%, and 100%) as well as Xylene and mounted in a

xylene-based mounting medium. Images were acquired using a ScanScope slide scanner (Aperio Technologies, Inc., Vista, CA). Quantitative size analysis of WAT adipocytes was performed using at least three images taken at 10× magnification for each group.

Electron microscopy

For TEM observation, WAT was cut into 1 × 2-mm blocks and fixed in 2.5% glutaraldehyde asl well as 1.5% PFA (in 0.1 M cacodylate buffer) for 30 min at room temperature. After fixation, samples were rinsed with deionized water, further fixed with 2% osmium tetroxide and 0.8% FeCN for 2 h, and washed with deionized water. Subsequently, the blocks were dehydrated in a series of graded ethanol (50%, 75%, 95%, and 100%) and acetonitrile, followed by embedding in Epon generic resin. Ultra-thin sections at a thickness of 90 nm were cut and stained with uranyl acetate and lead citrate. Stained sections were examined under a Tecnai T12 TEM attached with a Gatan imaging system (Gatan, Pleasanton, CA, USA).

For SEM examination, WAT was fixed with 2.5% glutaraldehyde and 1.5% PFA (in 0.1 M cacodylate buffer) for 1 h at room temperature, rinsed with deionized water, fixed with 1% osmium tetroxide for another 1 h, and washed with deionized water. After fixation, samples were dehydrated in a series of graded ethanol (50%, 70%, 85%, 95%, and 100%), critical-point dried, and observed under a Quanta 3D FEG Dual-beam SEM (FEI, Hillsboro, OR, USA).

Statistical analysis

All studies were performed in triplicate and data points are represented as mean values plus or minus standard error of the mean (mean ± SEM). To determine statistical significance, analysis of variance (two-tailed Student's t-test or ANOVA test) was performed using GraphPad Prism 7. Differences were considered statistically significant if $p \leq 0.05$.

SUPPLEMENTAL REFERENCE

Jiang, C., Cano-Vega, M.A., Yue, F., Kuang, L., Narayanan, N., Uzunalli, G., Merkel, M.P., Kuang, S., Deng, M., 2017. Dibenzazepine-Loaded Nanoparticles Induce Local Browning of White Adipose Tissue to Counteract Obesity. Mol. Ther. 25, 1718–1729.